

N 6 4 10 6 2 5

3 559606

GENERAL MILLS, ELECTRONICS DIVISION

Aerospace Research

2003 East Hennepin Avenue
Minneapolis 13, Minnesota

Inc., Minneapolis, Minn. CDP E-1 min. 2nd.

(NASA CR-52534)

OTS: \$2.60 phr, \$110 m²

T

INVESTIGATION OF SPUTTERING EFFECTS
ON THE MOON'S SURFACE

TS

Second Quarterly Status Report,
(NASA Contract NASw-751)

Covering Period 25 July 1963 to 24 October 1963

Submitted to:

National Aeronautics and Space Administration
Attention: Chief, Lunar and Planetary Programs
Office of Space Sciences
Washington 25, D.C.

Prepared by:

G. K. Wehner,

D. L. Rosenberg, and

C. E. KenKnight

Nov. 12, 1963 30-p ref

Submitted by:

G. K. Wehner

Assistant Director
Aerospace Research

Approved by:

Sam P. Jones, Director
Aerospace Research

Report No. 2476

Date: 12 November 1963

Project: 89308

INVESTIGATION OF SPUTTERING EFFECTS
ON THE MOON'S SURFACE

Second Quarterly Status Report
Contract NASw-751

ABSTRACT

10625

Experiments to investigate the influence of sputtering of the lunar surface by the solar wind were continued. Enrichment of metal concentration in surface layers of metallic oxides under hydrogen and mercury bombardment was demonstrated by x-ray scattering from the powders. An optical device for measurement of powder reflectivities is described and employed to measure the reflectivity of various materials. Powder surfaces sputtered under normal ion incidence are changed toward better agreement with the lunar results. Most surfaces are simultaneously darkened, in agreement with the low lunar albedo. Crusts of copper oxides after sputtering had high electrical conductivity. Build-up of copper oxide crusts from falling powder during sputtering resulted in cementing not otherwise observed. Sputtering of Fe, Ni, and Au wires by mass-analyzed beams of hydrogen molecular ions support the theoretically-expected sec θ dependence upon angle of incidence for 2 to 4 keV protons.

AUTHOR

an excellent summary article "Nature of the Lunar Surface" by
V. V. Sharonov.

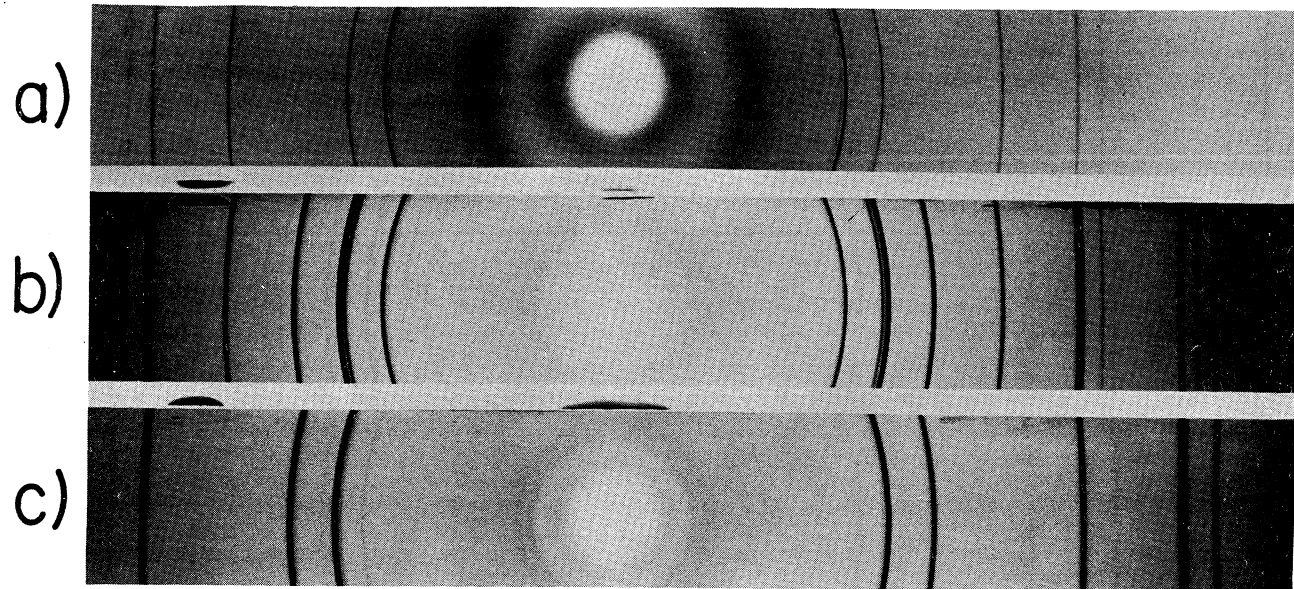
Experiments and topics to be discussed in this report are:

- (1) chemical change in sputtered surfaces,
- (2) the photometric properties of these surfaces,
- (3) the electrical conductivity of these surfaces,
- (4) crust build-up, and
- (5) angle of ion incidence studies.

II. X-RAY ANALYSIS OF SPUTTERED SURFACES

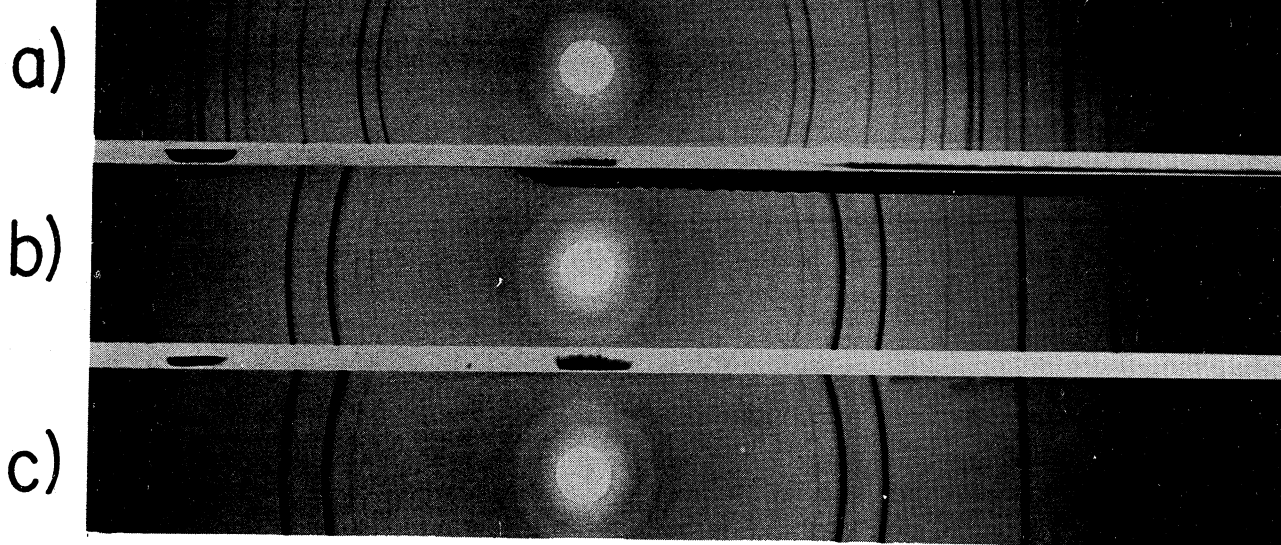
The metal enrichment of sputtered powder surfaces was briefly mentioned in a previous status report.⁹ The crusts formed on various powdered and granular material have been analyzed by the powder method of x-ray diffraction using Cu-K α radiation. In Figs. 1-3 the upper x-ray picture is of the original material, the middle picture is of the hydrogen sputtered material, and the lower is of the pure parent metal.

Figure 1, (Cu_2O), shows that the sputtered surface is composed of Cu_2O and Cu in comparable proportions. Under visual examination the spires appear metallic but the overall color is that of darkened Cu_2O . A similar x-ray analysis of a mercury ion bombarded Cu_2O surface reveals much less Cu although the total amount of physical sputtering of the surface is greater than with hydrogen. This illustrates the enhancement of the physical sputtering effect by chemical reaction with the reducing ion. The deposits of sputtered material on the glass shields and on the inner wall of the target material container appear to be pure copper. This is true with both hydrogen and mercury sputtering. This indicates that the molecules are disassociated in the sputtering



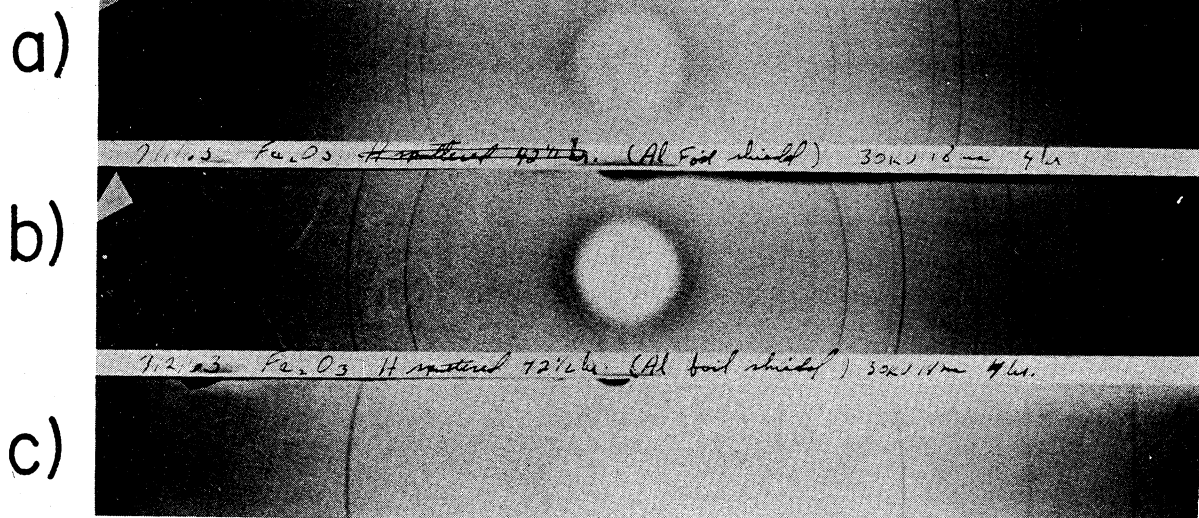
- a) Cu_2O powder
- b) Hydrogen sputtered Cu_2O powder
- c) Copper

Fig. 1 Powder x-ray analysis of hydrogen sputtered Cu_2O powder.



- a) CuO powder
- b) Hydrogen sputtered CuO powder
- c) Copper

Fig. 2 Powder x-ray analysis of hydrogen sputtered CuO powder.



- Fe_2O_3 powder
- Hydrogen sputtered Fe_2O_3 powder
- Iron

Fig. 3 Powder x-ray analysis of hydrogen sputtered Fe_2O_3 powder.
(Aluminum foil used as x-ray film shield.)

and that oxygen atoms must have a lower sticking probability. Figure 2, (CuO), indicates that the crust is almost all copper and only traces of CuO and Cu_2O are detectable. There was no indication of CuO in the sputtered Cu_2O surface. In the case of CuO , the action of the hydrogen plasma alone will turn the surface metallic in several minutes of exposure but no crust is formed unless the target is sputtered. With mercury ion sputtering of CuO , the x-ray analysis indicates roughly equal proportions of CuO and Cu. Figure 3, (Fe_2O_3), indicates the sputtered surface contains Fe_2O_3 and Fe, but also one or more other constituents which have not been determined.

Powder x-ray analyses of basalt, pumice, and scoria surfaces have not shown detectable changes in composition of the surface due to sputtering. The sensitivity of our technique is probably not high enough for these minerals. We expect metal enrichment is still present but not to the extent it is in copper and iron oxides.

III. PHOTOMETRIC PROPERTIES OF ION BOMBARDED SURFACES

Surface darkening and the enhancement of backscattering were noted in our earlier studies of sputtered powders. To study this more quantitatively, a "reflectometer" was fabricated (see Fig. 4). A horizontal target surface can be illuminated and viewed from angles of -90° to $+90^\circ$. The target is illuminated with a Bausch and Lomb microscope illuminator head using a General Electric No. 1630 spiral filament bulb at reduced voltage. The light beam is formed by a two-lens system and reflected 90° by a front surface mirror onto the target. This mirror arrangement

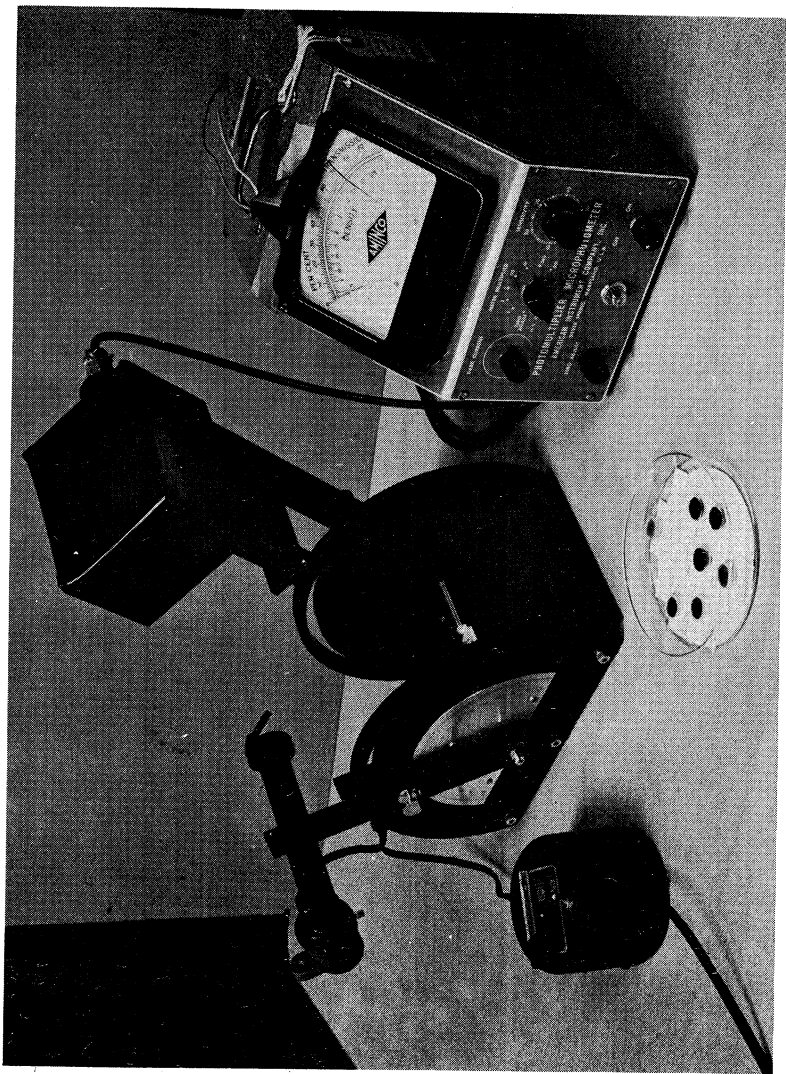


Fig. 4 Reflectometer used to measure reflection characteristics of sputtered powder surfaces.

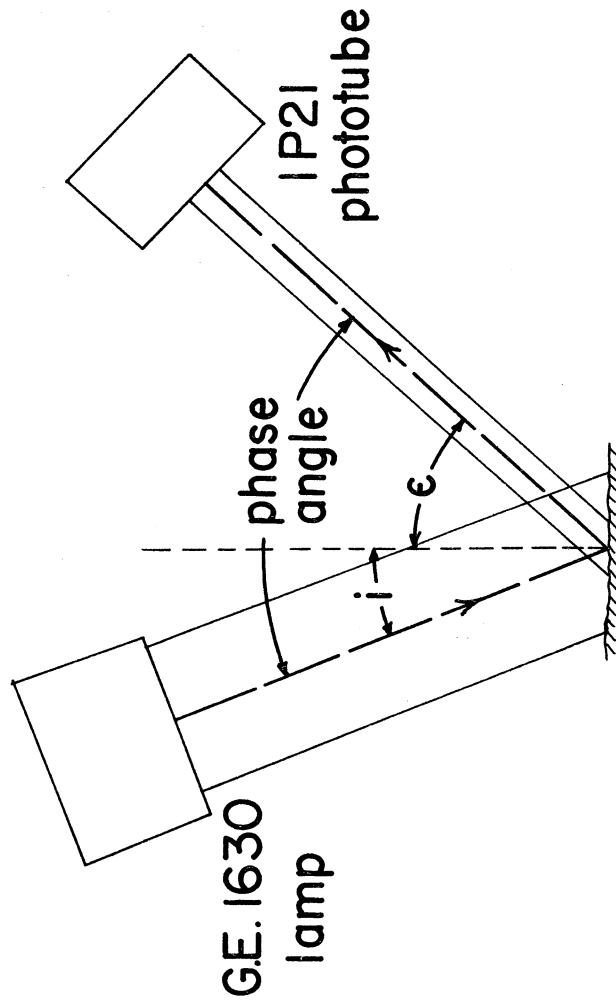


Fig. 5 Optical system of reflectometer.

allows measurements to be made at phase angles down to $2\frac{1}{2}^\circ$. (The phase angle is the angle between the angle of illumination, i , and the angle of detection, ϵ .) The minimum phase angle of the lunar surface as measured from the earth is approximately $1\frac{1}{2}^\circ$. The beam spot is 17 mm in diameter at the target stage. The detector system employs a 1P21 phototube and one lens and sees a 3 mm diameter spot on the target surface when the detector is normal to the surface (angle of detection 0°). Figure 5 is a schematic of this optical system. Eastman Kodak Neutral Density Filters are used in the reflected light path when measuring the lighter colored samples. The phototube is usually operated at its lowest sensitivity range even for a relatively dark sample; the use of a neutral density filter assures a constant color temperature of the illumination.

Reflection curves are determined for each surface before and after sputtering. The sputtered surface is measured as soon after removal from the discharge tube as is conveniently possible to minimize changes due to the action of the atmosphere. Mercury ion sputtered alumina darkened considerably within several days after removal. Six scans are made of each surface. In three, the angle of illumination is fixed at 0° , 30° , and 60° and ϵ varied from -80° to $+80^\circ$ in 10° intervals with measurements also made at phase angles of $\pm 5^\circ$ and $\pm 2\frac{1}{2}^\circ$. Plotting these data on polar coordinates allows comparison of our results with those of Orlova.¹⁰ The last three scans are made in a like manner except ϵ is fixed and i is varied. Presented this way, our results can be compared with those of Hapke and VanHorn.⁶

The approximate hydrogen ion current density in our system is 1.7 mA/cm^2 . Assuming a solar-wind density of $2 \times 10^8 \text{ ions/cm}^2 \text{ sec}$ and a factor of 2 to account for lunar day and night, one hour of laboratory sputtering is equivalent to 12,000 years on the Moon or 90 hours in the laboratory to one million years on the Moon. The mineral targets were sputtered for ~ 90 hours and the oxide targets for ~ 40 hours.

The reflection curves given in Figs. 6 and 7 are of yellow sand and lichen. The lichen curves, from Hapke and VanHorn's work,⁶ follow the lunar curve quite closely, while our sand curve is more that of a Lambertian reflector with some backscatter. All angles in the curves are measured from the normal. Figures 8 and 9 are of sputtered and unspattered Cu_2O . This surface was described and pictured in the first status report of this contract. Our original surfaces are poured before measuring and before sputtering. A surface formed by sifting has a more pronounced backscatter. The original surface has a pronounced backscatter but it is less than that of the Moon. The hydrogen sputtered surface has a more pronounced backscatter than that of the Moon. The reflection curves for basalt with $2\text{-}10 \mu$ particle size are shown in Figs. 10 and 11. In this case the reflection curve of the original powder surface is similar to that of sand. On sputtering with hydrogen ions ~ 90 hours, the reflection curve now closely resembles that of the Moon. R. J. P. Lyon¹¹ of Stanford Research Institute has studied various surfaces in the infrared region under a NASA contract. It would be interesting to have him study our sputtered surfaces in this region of the spectrum.

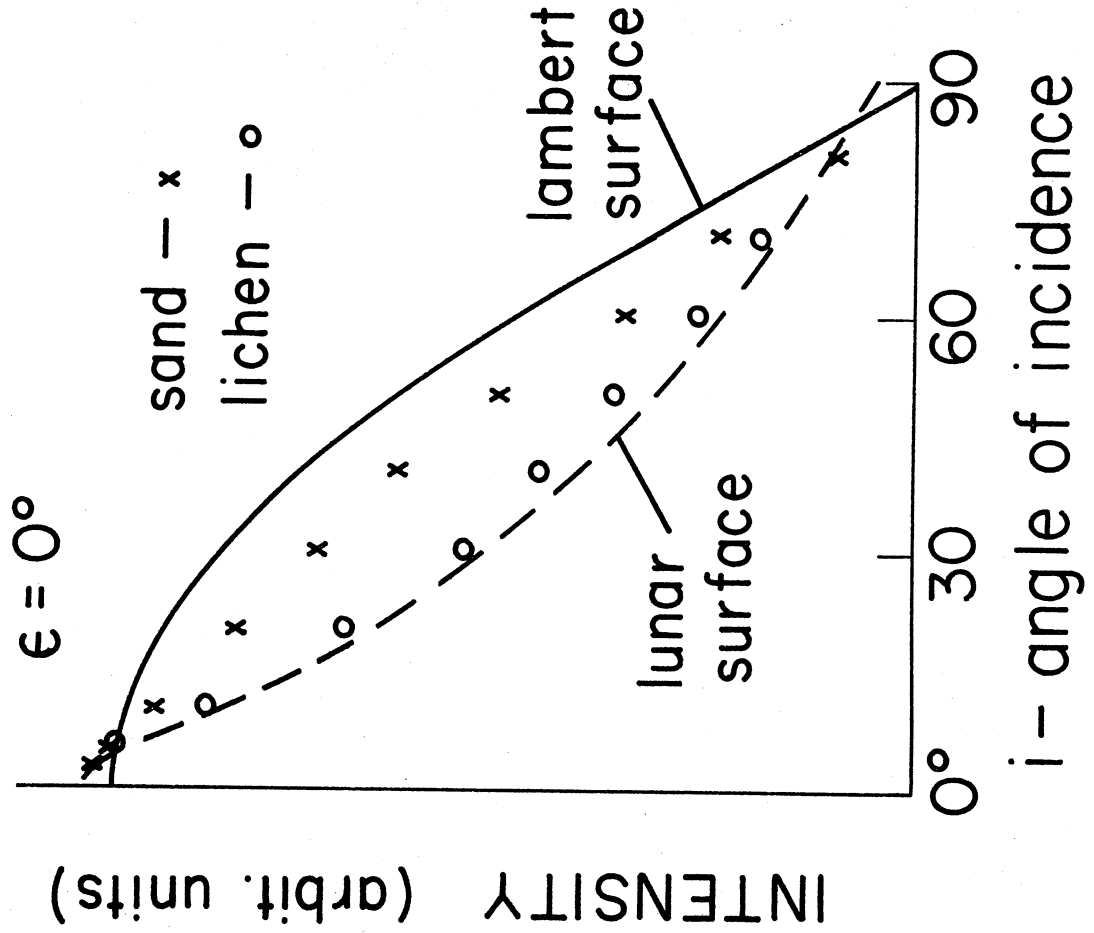


Fig. 6 Reflection curves in visible light for yellow sand and lichen.
All angles are measured from the normal. Angle of reflection, 0° .
(The lichen curve is from Reference 3.)

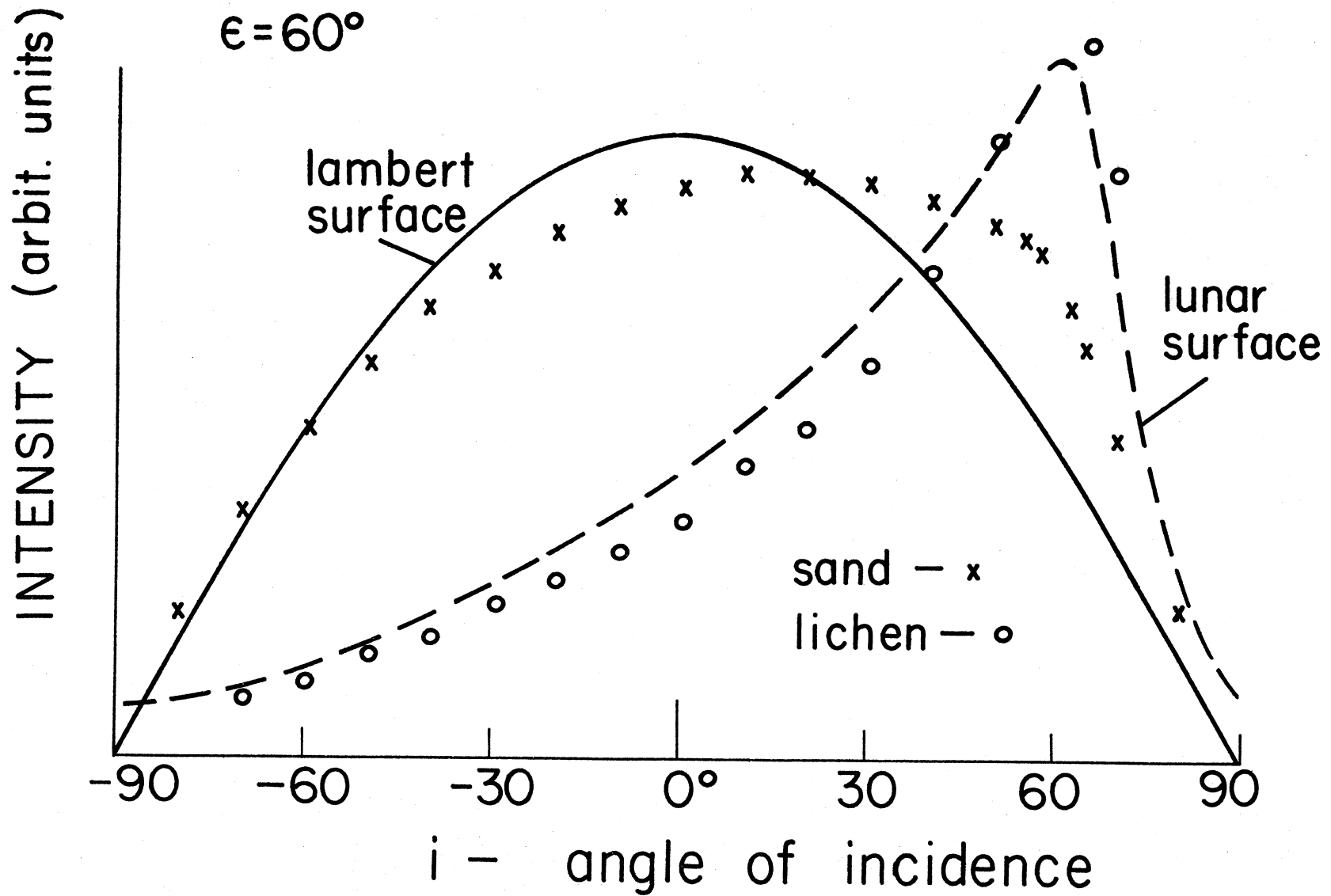


Fig. 7 Reflection curves in visible light for yellow sand and lichen. All angles are measured from the normal. Angle of reflection, 60° . (The lichen curve is from Reference 3.)

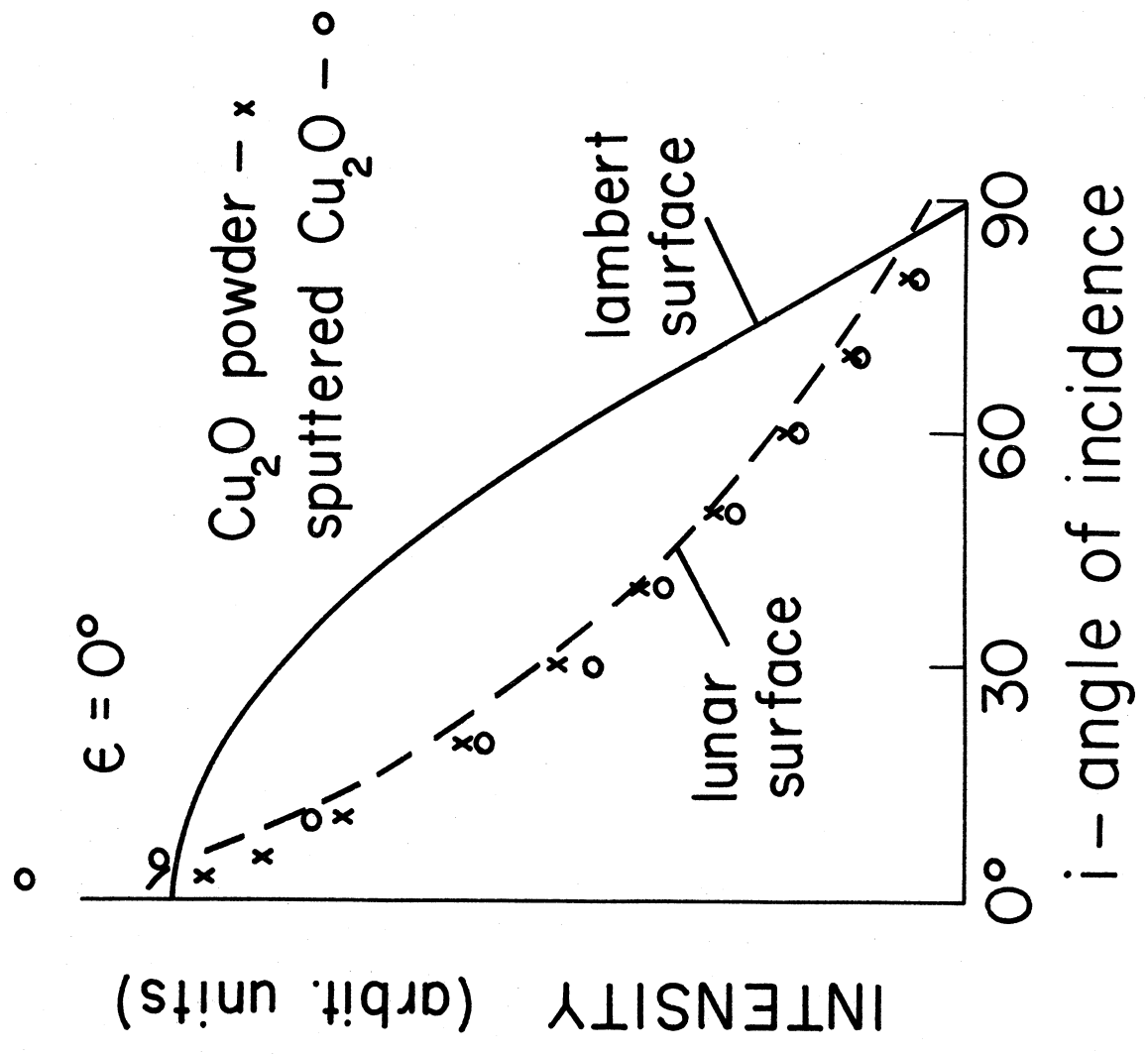


Fig. 8 Reflection curves in visible light for Cu₂O powder and a crust formed on Cu₂O powder by hydrogen sputtering for ~ 40 hours. Angle of reflection, 0° . All angles are measured from the normal.

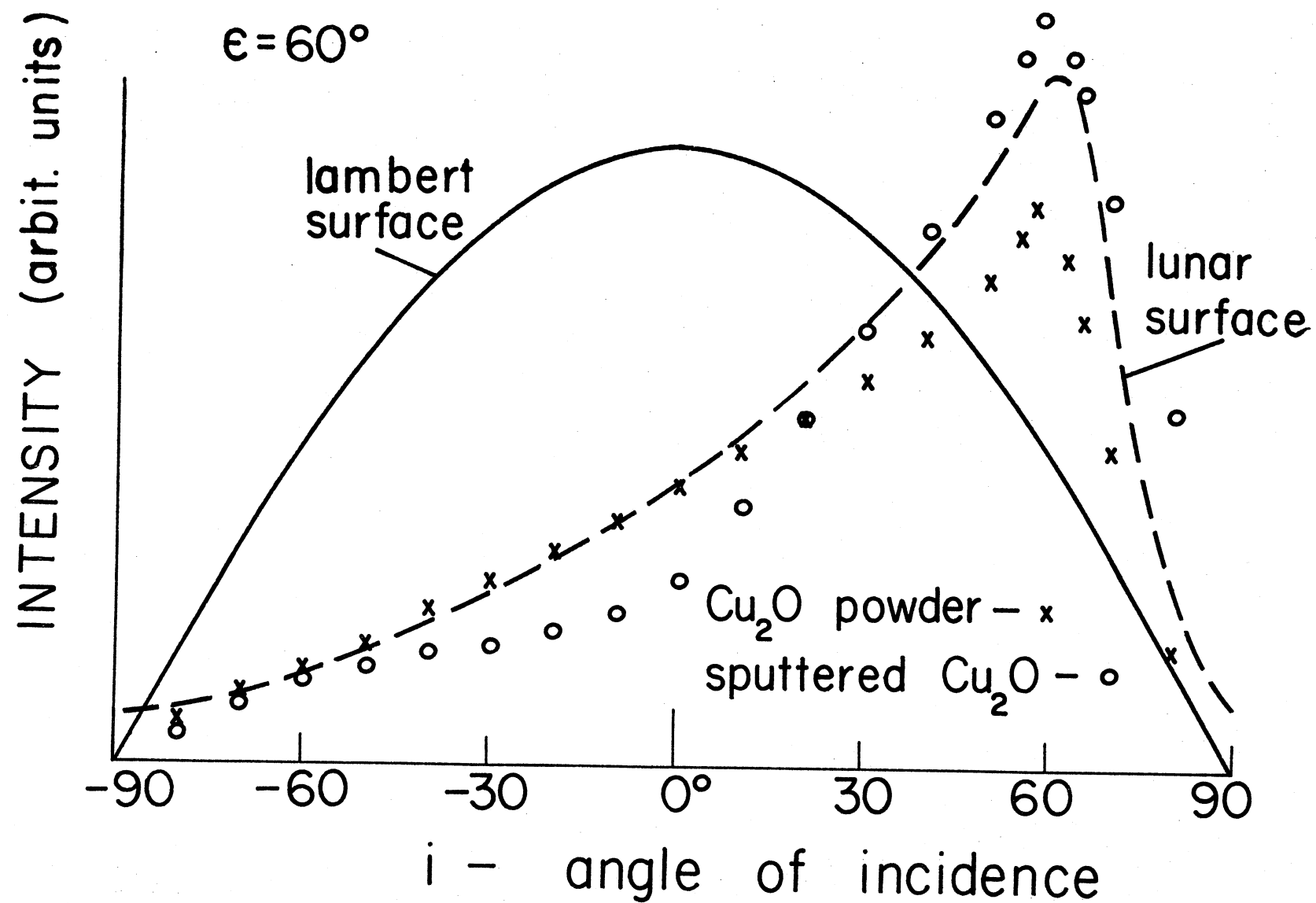


Fig. 9 Reflection curves in visible light for Cu_2O powder and a crust formed on Cu_2O powder by hydrogen sputtering for ~ 40 hours. Angle of reflection, 60° . All angles are measured from the normal.

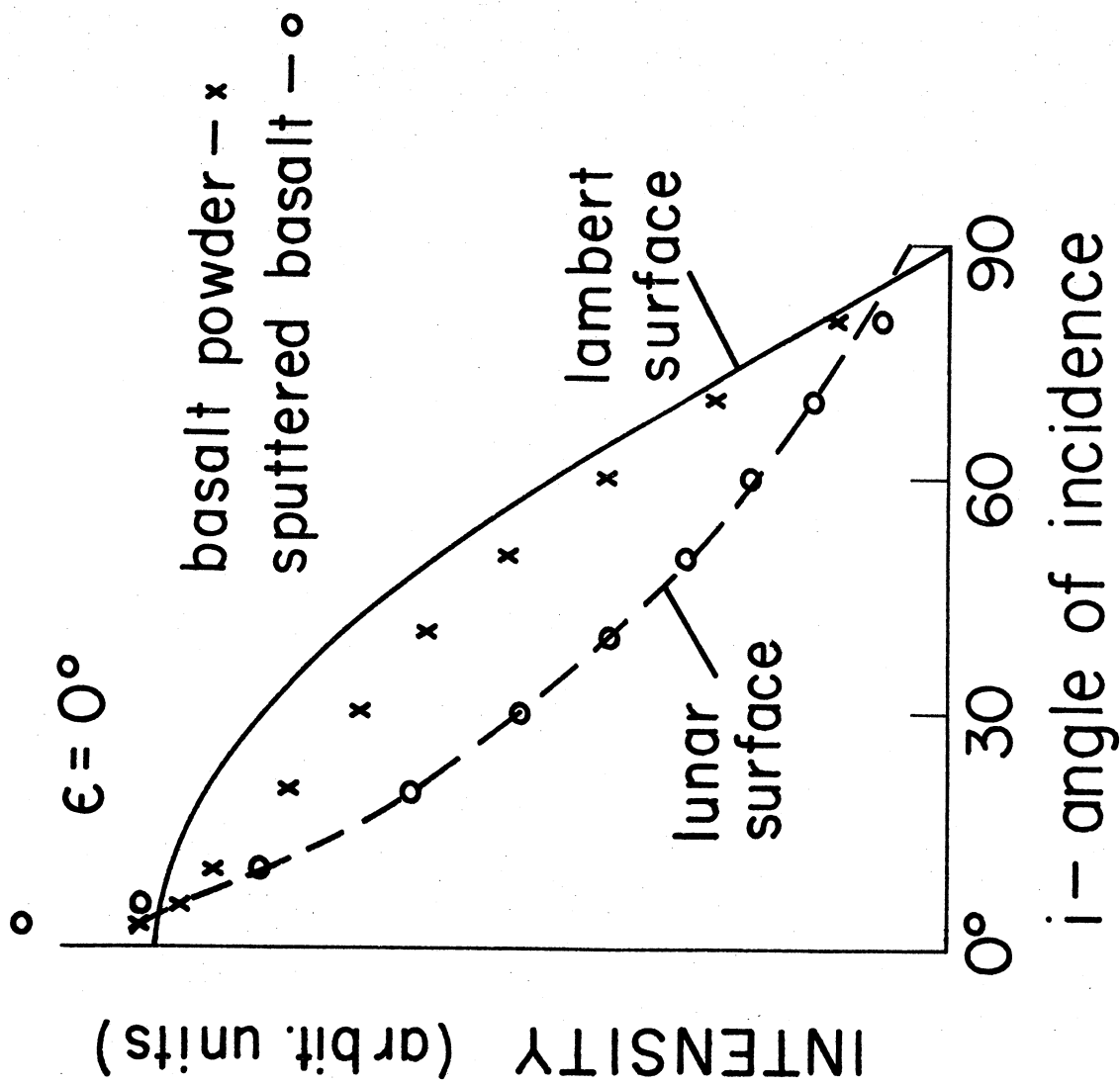


Fig. 10 Reflection curves in visible light for basalt powder and a crust formed on basalt powder by hydrogen sputtering for ~ 90 hours. Particle size of original powder, $2-10\mu$. Angle of reflection, 0° . All angles are measured from the normal.

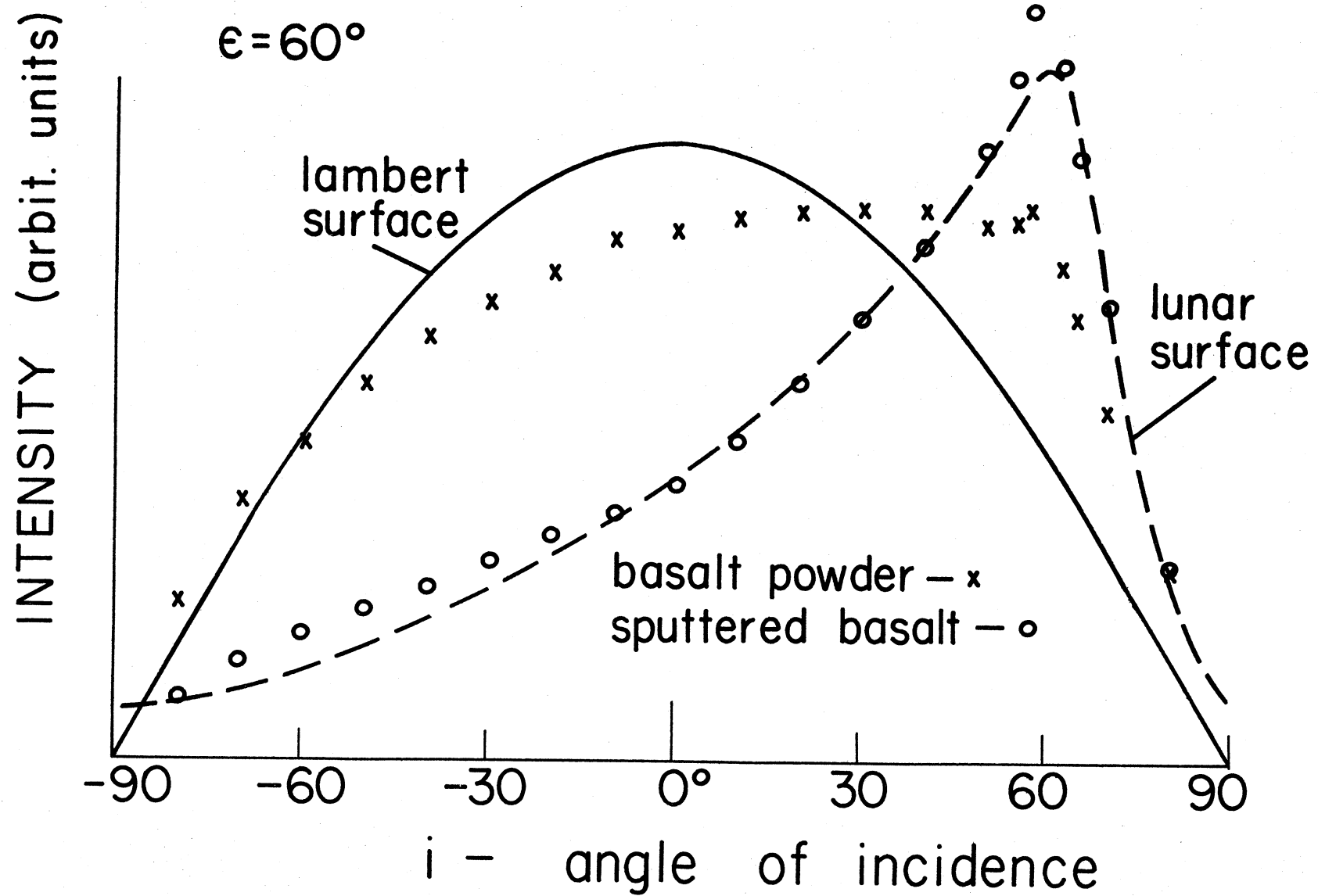


Fig. 11 Reflection curves in visible light for basalt powder and a crust formed on basalt powder by hydrogen sputtering for ~ 90 hours. Particle size of original powder, $2\text{-}10 \mu$. Angle of reflection, 60° . All angles are measured from the normal.

Hydrogen sputtering of powder surfaces in all cases studied increased the backscattering and darkened the surface in most cases. One exception to this darkening tendency is black CuO. After \sim 40 hours of sputtering, the originally flat and black surface became dome shaped with the center several millimeters above the original level and the entire surface was covered with irregular metallic copper spires pointing in a direction parallel to the bombarding ions. This actual "growing" of the surface will be studied further. This surface is an exaggeration of the general effect of sputtering both with respect to chemical reduction and formation of a spire-covered surface.

Figure 12 is a color photograph illustrating, although rather poorly, the darkening due to hydrogen sputtering. In each material pictured, an unspattered surface is at the left, the sputtered on the right. Alumina was only slightly darkened and, as mentioned above, CuO powder was lightened by almost total reduction to metallic copper.

Other materials and the same materials with other particle sizes will be sputtered in the future and the change of reflection characteristics as a function of sputtering time will be studied.

IV. ELECTRICAL CONDUCTIVITY OF SPUTTERED SURFACES

The electrical conductivities of crusts formed on Cu_2O and CuO powder by hydrogen and by mercury sputtering were measured. Measurements on mercury sputtered crusts were made in the sputtering vacuum system so as not to disrupt the contact between electrodes and crust. The initial resistance of Cu_2O was essentially infinite (> 5 megohms) but after 15 minutes of mercury sputtering the resistance dropped to 100,000 ohms per square; after four

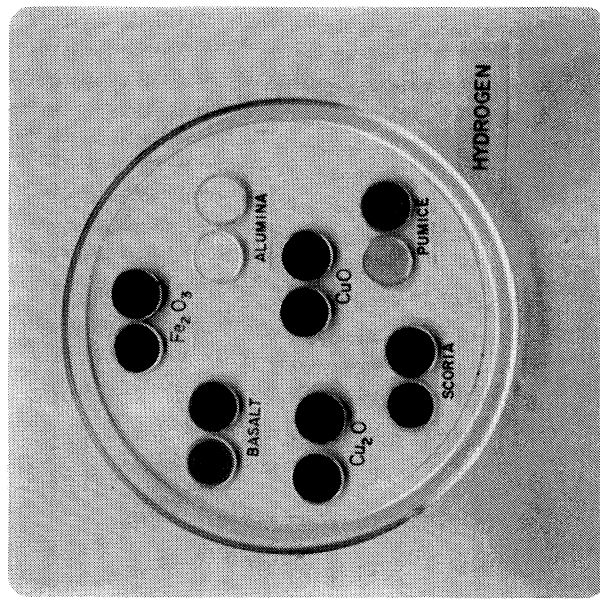


Fig. 12 Photograph of hydrogen sputtered materials illustrating darkening effect of sputtering. Unsputtered material is on the left.

hours it rose to approximately 300,000 ohms per square. On cooling the target several minutes, the resistance again increased to infinity. Similar results were obtained upon repeating the experiment. We feel the increase of resistance on cooling is due to loss of contact between electrodes and crust. After removal from the vacuum system, the sample was probed by hand and also by the use of two mercury droplets as electrodes. There was some indication of electrical conduction but the layer is so fragile that no reproducible values could be obtained.

The initial drop of the resistance after 15 minutes sputtering to less than the "steady state" value is probably significant. The surface has been reduced to copper but the spires have not yet been formed. The conduction path length should be longer in a surface covered with spires because the spires do not touch and they shield the Cu₂O underneath from reduction by sputtering.

With CuO sputtered by mercury, the resistance was 4000 ohms per square after 20 minutes of sputtering and remained essentially constant for 13 hours of sputtering.

Hydrogen sputtered Cu₂O and CuO crusts were not measured while in the sputtering system. On probing the Cu₂O crust after removal, the resistance between points several millimeters apart was of the order of tens of ohms. With a CuO crust, the resistance was of the order of several ohms. These findings are in line with our powder x-ray analysis results.

V. CRUST BUILD-UP

All crusts formed by sputtering a powder surface were one millimeter thick or less. An attempt was made to build up a thicker crust.

An automatic shaker device was set up allowing a small amount of Cu₂O powder to drop every six minutes onto a tantalum plate being sputtered by 250-eV mercury ions. After about 30 hours, a crust 7 mm high was built up. The crust was fragile but the cementation was adequate to allow the plate to be inverted without losing the crust. A control was run to check the possibility that the action of the plasma was responsible for the cementation. In this case the powder fell off when the plate was tilted about 60°, showing that the sputtering cementation substantially increases the strength of the crust.

VI. ANGLE OF INCIDENCE DEPENDENCE IN SPUTTERING BY HYDROGEN IONS

The sputtering yield for ions incident on a smooth, convex, polycrystalline solid surface should be a monotonically increasing function of the angle of incidence θ , measured from the normal. At more oblique incidence, the incident atoms penetrate less deeply into the lattice so that the transport of momentum to the surface is more probable. It can be shown that the sputtering yield $Y(\theta)$ is related to the erosion rate along the beam direction $Z(\theta)$ by a simple constant of proportionality:

$$Y(\theta) = \frac{e}{j} \cdot \frac{\rho}{m} Z(\theta)$$

where j is the ion beam current density (which can be assumed constant near the beam center for a small target), ρ is the density of the target,

and m the mass of the target atoms. In using this relation to infer the angular dependence of the sputtering yield it is important that the surface be convex so that the sputtered atoms are not condensed elsewhere on the same sample and that the direction of the surface normal be well defined despite the local roughness due to crystallites.

In previous work in this laboratory¹² spheres of various metals were placed in beams of Hg^+ at about 10 keV. Cross sections were photographed in a projection microscope before and after exposure to the beam. In that apparatus it was possible to arrange several beams so that a number of spheres could be bombarded per opening of the vacuum system.

In this work, wires of Fe, Ni, and Au were placed in beams of H_2^+ or H_3^+ at about 5 keV. Advantage was taken of the variation in current density of the beam along the length of the wire; various cross sections of the wire experienced different amounts of erosion. By comparing photographs like that of Fig. 13 for several adjacent cross sections, several curves for $Y(\theta)$ can be obtained from a single wire.

The statistical significance of an averaged curve is thereby increased. The wire is much smaller than the transverse dimensions of the beam so that the assumption of constant ion current density over a wire cross section is justified. Typically, the wires were 0.10 mm in diameter and the beam diameter five times larger.

The sputtering theory of Goldman and Simon¹³ is that of fast light ions on heavy atoms and may be expected to be valid here. They predict a dependence of yield upon angle of incidence as $\sec \theta$. In that case the incremental erosion of a circular cross section is particularly

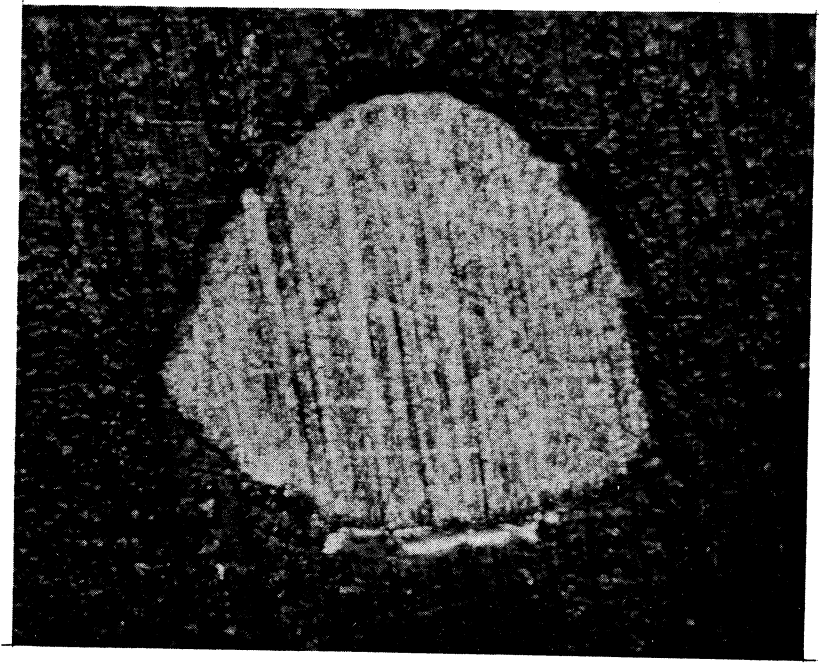
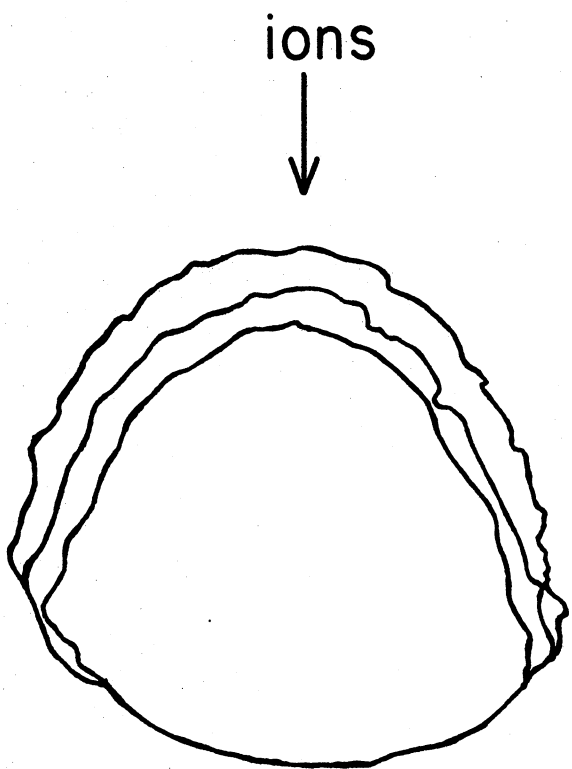


Fig. 13 Photograph of 0.005 in. Au wire, sectioned in clear plastic and etched 1 minute in aqua regia, 380x in metallographic microscope.

simple because $\dot{Z} = \dot{r} \sec \theta$ so that the erosion in the radial direction is constant on the interval $0 \leq \theta < 90^\circ$. The final cross section of the wire would be the intersection of a section of the original circle with a half-circle of smaller radius.

The experimental results for Fe, Ni, and Au corroborate the $\sec \theta$ dependence to about $\theta = 70^\circ$. Above 70° , the erosion rate $\dot{Z}(\theta)$ becomes more nearly constant, though this region is very difficult and large uncertainties are the rule. According to the simple picture presented above, the limiting angle of incidence would be 90° . In practice, the wire has a finite roughness due to the crystallites. As a result, the limiting effective angle of incidence is less than 90° . As the rising Sun illuminates only the sides of high mountains, so the ion beam sputters only surfaces tilted from the local tangent plane. The specific cases studied were 7 keV H_2^+ on Fe, 6.0 keV H_3^+ on Ni, and 8.0 keV H_2^+ on Au. Tracings of the wire profiles from photographs of the Au wire cross sections are presented in Fig. 14. The waviness of the profiles indicates the effect of finite crystallite size.

We conclude that the evidence for a $\sec \theta$ dependence of the sputtering yield as a function of angle of incidence is supported by experiment for Fe, Ni, and Au. The validity of considering a molecular ion as several independent protons is discussed elsewhere.^{1,14} These results, then, are applicable to protons of 2-4 keV. Since the current density depends upon angle of incidence as $\cos \theta$, the sputtering rate normal to the surface of the Moon should be independent of the angle of proton



8 kev H_2^+ on Au wire

Fig. 14 Tracings of Au wire cross sections separated by about 0.008 in. along the wire. Bombardment by 8 keV H_2^+ ions in a beam of diameter about 0.140 in.

incidence. The sputtering rate is proportional to the product of current density and the sputtering yield.

LIST OF REFERENCES

1. Wehner, G. K., C. E. KenKnight, and D. L. Rosenberg. Sputtering rates under solar-wind bombardment. *Planetary Space Sci.* 11: 885-95 (1963).
2. ----, ----, and ----. Modification of the lunar surface by the solar-wind bombardment. To be published in *Planetary Space Sci.*
3. Bonetti, A. et al. Explorer 10 plasma measurements. *J. Geophys. Res.* 68: 4017-63 (1963).
4. Snyder, C. W. and M. Neugebauer. Interplanetary solar-wind measurements by Mariner II. Presented at Symposium on Plasma Space Science, Washington, D.C., June 1963.
5. Whipple, F. L. Meteoritic erosion in space. In *Air Force Cambridge Research Laboratories. Geophysical Research Papers No. 75. Proceedings of the Symposium on the Astronomy and Physics of Meteors*, 28 Aug. - 1 Sept. 1961. pp. 239-48.
6. Hapke, B. and H. Van Horn. Photometric studies of complex surfaces, with applications to the moon. *J. Geophys. Res.* 68: 4545-70 (1963).
7. ----. A theoretical photometric function for the lunar surface. *J. Geophys. Res.* 68: 4571-86 (1963).
8. Barabashov, N. P., V. A. Bronshten, et al. The moon. Moscow, Litratury State Publishing House of Physics - Mathematical Literature, 1960.
9. General Mills, Inc. Electronics Group. Report 2308. Sputtering effects on the moon's surface, by G. K. Wehner. Contract NASw-424. First Quart. Status Report (18 July 1962).
10. Orlova, N. S. Photometrical relief of the lunar surface. *Astron. Zh.* 33, 1: 93-100 (1956).

LIST OF REFERENCES (Cont'd.)

11. Stanford Research Institute. Evaluation of infrared spectrophotometry for compositional analysis of lunar and planetary soils, by R. J. P. Lyon. Contract NASr-49(04). Quart. Status Report no. 5 (Sept. 1963).
12. Wehner, G. K. Influence of the angle of incidence on sputtering yields. J. Appl. Phys. 30: 1762-65 (1959).
13. Goldman, D. T. and A. Simon. Theory of sputtering by high-speed ions. Phys. Rev. 111: 383-86 (1958).
14. KenKnight, C. E. and G. K. Wehner. Sputtering of metals by hydrogen ions. Accepted for publication by J. Appl. Phys.

LIST OF ILLUSTRATIONS

Fig. 1 Powder x-ray analysis of hydrogen sputtered Cu_2O powder.

Fig. 2 Powder x-ray analysis of hydrogen sputtered CuO powder.

Fig. 3 Powder x-ray analysis of hydrogen sputtered Fe_2O_3 powder.
(Aluminum foil used as x-ray film shield.)

Fig. 4 Reflectometer used to measure reflection characteristics of sputtered powder surfaces.

Fig. 5 Optical system of reflectometer.

Fig. 6 Reflection curves in visible light for yellow sand and lichen.
All angles are measured from the normal. Angle of reflection, 0° .
(The lichen curve is from Reference 6.)

Fig. 7 Reflection curves in visible light for yellow sand and lichen.
All angles are measured from the normal. Angle of reflection, 60° .
(The lichen curve is from Reference 6.)

Fig. 8 Reflection curves in visible light for Cu_2O powder and a crust formed on Cu_2O powder by hydrogen sputtering for ~ 40 hours.
Angle of reflection, 0° . All angles are measured from the normal.

Fig. 9 Reflection curves in visible light for Cu_2O powder and a crust formed on Cu_2O powder by hydrogen sputtering for ~ 40 hours.
Angle of reflection, 60° . All angles are measured from the normal.

Fig. 10 Reflection curves in visible light for basalt powder and a crust formed on basalt powder by hydrogen sputtering for ~ 90 hours.
Particle size of original powder, $2\text{-}10 \mu$. Angle of reflection, 0° .
All angles are measured from the normal.

LIST OF ILLUSTRATIONS (Cont'd.)

Fig. 11 Reflection curves in visible light for basalt powder and a crust formed on basalt powder by hydrogen sputtering for ~90 hours. Particle size of original powder, 2-10 μ . Angle of reflection, 60°. All angles are measured from the normal.

Fig. 12 Photograph of hydrogen sputtered materials illustrating darkening effect of sputtering. Unspattered material is on the left.

Fig. 13 Photograph of 0.005 in. Au wire, sectioned in clear plastic and etched 1 minute in aqua regia, 380x in metallographic microscope.

Fig. 14 Tracings of Au wire cross sections separated by about 0.008 in. along the wire. Bombardment by 8 keV H₂⁺ ions in a beam of diameter about 0.140 in.